

Effect of Load Models on the Optimal Allocation of Solar and Wind Distributed Generation Using Stochastic Approach

Rodolfo A. Aguirre, Jr.^{1*}, Rei-Ann M. Dayapera¹, and Carl Peter Christian C. Caampued¹

¹Department of Electrical Engineering, College of Engineering and Agro-Industrial Technology, University of the Philippines Los Baños, 4031 Los Baños, Laguna

* Corresponding author (raaguirre@up.edu.ph)

Received, 12 November 2018; Accepted, 15 June 2019; Published, 19 July 2019

Copyright © 2019 R.A. Aguirre, Jr., R.M. Dayapera, & C.P.C.C. Caampued. This is an open access article distributed under the Creative Commons Attribution License, which permits unrestricted use, distribution, and reproduction in any medium, provided the original work is properly cited.

Abstract

Integration of renewable type of distributed generation (DG) system specifically solar and wind has provided multiple benefits including positive environmental impact. However, improper allocation may result in increased voltage fluctuations and system losses. In this paper, comparison of optimal allocation for different solar and wind DG scenarios based from loss reduction and voltage improvement was made. DG and load models were considered to determine their effect in the distribution network. Simulations were implemented to IEEE 37-bus test system using Genetic Algorithm in the Component Object Model interface of MATLAB and OpenDSS. The study shows that the integration of both solar and wind DGs with constant power factor lagging model resulted in the most significant improvement in a system with commercial load model.

Keywords

Optimization of wind and solar DGs, renewable distributed generation, solar DG modeling, wind DG modeling, genetic algorithm, MATLAB, OpenDSS

Introduction

Through the years, electric power system has been facing major challenges due to increasing load demand in the network, mainly by electricity utilization of residential and commercial buildings [1]. In the Philippines, these loads contributed to 1.83% increase in energy consumption during the first half of 2017 [2]. With the development in the residential and commercial sectors, utilities may need to build additional generation facilities to meet the growing demand which will require large cost. Consequently, prices of fossil fuels needed to run conventional power plants has been increasing rapidly due to the degradation

of its supply [3]. These existing problems require electric system operators to provide power in a way far from the traditional one, which requires continuous supply of oil and natural gas. One possible solution is the integration of renewable energy resources [2,3].

Distributed generation (DG) is a generator that is placed near the consumers [4]. Commonly, DG has an output power of up to 50 MW [5]. It is usually classified into two types, namely renewable and non-renewable. Despite having intermittency as a drawback, renewable type is still a viable option due to the mitigation of adverse environmental impacts as compared to the non-renewable type [6]. Some of the examples

of renewable type include biomass, geothermal, hydro, wind, and solar [7]. At planning stage, proper siting can be an issue for both geothermal and hydro DGs because both types are site-specific. For biomass, environmental and health issues are the concerns at operation stage. For these reasons, solar and wind are among the popular renewable DG nowadays.

Solar DG is gaining an advantage in the development of renewable energy due to its significant cost reduction. For almost a decade, there is approximately 80% decrease in the prices of solar PV modules globally [8]. On the other hand, wind DGs are often injected into the system because of its reactive power control capabilities which can be used to mitigate voltage fluctuations [9]. Furthermore, unlike other renewable DGs, both technologies are relatively easier to locate since they can either be roof- or ground-mounted. Integration of renewable DG will force the power system to shift from the traditional centralized network consisting of large power plants to a more decentralized one. DG, as compared to traditional plants, is relatively smaller which is easier to install with reduced maintenance cost [5].

Generally, DG provides benefits to consumers especially in areas where traditional plants are deemed impractical [4]. Since load demand can be met accordingly, the need for additional investments on transmission and distribution facilities is reduced [10]. However, inappropriate allocation in terms of size and site can reverse power flow. Reversed power flow can increase voltage and short circuit currents in the distribution area which can damage protective and control devices [6]. Furthermore, it can increase power loss and fluctuations in the voltage profile. Therefore, optimal allocation is very crucial to maximize the benefits of DG integration such as power quality improvement and voltage stability [10].

To address this problem, many optimization tools have been presented, which may have a single or multi-objective function. Some of the most common objective functions include power loss reduction and voltage profile improvement [5, 9–11]. In the renewable DG integration, inclusion of stochastic data has a great impact on allocation which, if not properly modelled, may result in non-optimal solution

[12]. Furthermore, non-inclusion of stochastic data may lead to overestimation of the positive impacts of the allocation of DGs such as loss reduction and voltage improvement. Moreover, proper modelling of generator should also be integrated in allocation studies to consider the reactive control capabilities of DGs. It was observed in studies that among the DG models, constant lagging power factor (pf) model had the most significant improvement in terms of voltage profile and power loss [12, 13]. Despite improving the optimal allocation of DG, most of the works had modelled the load as constant power. Comparing to the works involving the integration of DG in a system, only a few have presented studies on optimal allocation with different load models. Majority of the works failed to consider the effects of load models which could lead to misleading results due to the underestimation of the actual type of loads utilized by the consumers. In addition, load models either classified as residential and commercial can affect the capacity and location of DG [14]. These loads are also known as voltage-dependent loads because real and reactive powers are significantly affected by voltage variation. It was presented in a study that voltage-dependent load models affect the voltage profile and power loss of the distribution system [15]. Therefore, load models should be incorporated in studying optimal allocation of DG.

Another thing to consider is that solar and wind DGs both use power inverters which can generate reactive power. Management of reactive power in the distribution system is an important process in controlling the voltage level [16]. Reactive power can either be generated or absorbed to increase or decrease the voltage of the system, in order to reduce thermal loss and to balance load distribution.

At present, there are no existing methods that consider the effect of residential and commercial load models in the context of optimal sizing and siting of various solar and wind DG models in a distribution network. The exclusion of the type of loads in the allocation of DG could lead to concerns regarding sub-optimal results. To address this issue, it is necessary to conduct a study that integrates the load models in the optimal allocation of renewable DGs using stochastic approach.

Materials and Methods

The implementation of DG optimal allocation is composed of two parts, namely, the network parameter modelling and the optimization method. The first part includes different solar DG, wind DG, and voltage-dependent load models. The second part comprises the optimization algorithm and the load flow implementation.

Solar DG Modelling

In the modelling of solar DG, the intermittency of the solar irradiance was taken into account for the power output. In addition, the unity, constant, and variable lagging power factor models of reactive power control for solar DG were considered for comparison.

A. Beta Distribution of Solar Irradiance

One of the factors that significantly affect the solar DG power output is the solar irradiance which follows the Beta probability density distribution [17]. The Beta distribution is defined using the following equation:

$$f_b(s) = \begin{cases} \frac{\Gamma(\alpha + \beta)}{\Gamma(\alpha) \Gamma(\beta)} * s^{(\alpha-1)} * (1-s)^{(\beta-1)}, & \text{for } 0 \leq s \leq 1, \alpha \geq 0, \beta \geq 0 \\ 0, & \text{otherwise} \end{cases} \quad (1)$$

where s is the solar irradiance in kW/m^2 , $f_b(s)$ is the beta distribution of the function of s , α is the shape parameter, and β is the size parameter. For the calculation of the shape and size parameters of the random variable s , the following formula will be used:

$$\beta = (1 - \mu) * \left(\frac{\mu * (1 + \mu)}{\sigma^2} - 1 \right) \quad (2)$$

$$\alpha = \frac{\mu * \beta}{1 - \mu} \quad (3)$$

where μ is the mean, and σ is the standard deviation.

Together with the solar irradiance per hour, the solar DG power output is also dependent on the module characteristics as defined in the following formula:

$$T_c = T_A + s * \left(\frac{N_{OT}-20}{0.8} \right) \quad (4)$$

$$I = s * [I_{SC} + K_i (T_c - 25)] \quad (5)$$

$$V = V_{OC} - K_v * T_c \quad (6)$$

$$P_s(s) \quad (7)$$

$$FF = \frac{V_{MPP} * I_{MPP}}{V_{OC} * I_{SC}} \quad (8)$$

where T_c is the cell temperature in $^{\circ}\text{C}$, T_A is the ambient temperature in $^{\circ}\text{C}$, K_v is the volt temperature coefficient in $\text{V}/^{\circ}\text{C}$, K_i is the current temperature coefficient in $\text{A}/^{\circ}\text{C}$, N is the nominal operating temperature of cell in $^{\circ}\text{C}$, FF is the fill factor, I_{SC} is the short circuit current in A, V_{OC} is the open-circuit voltage in V, I_{MPP} is the current at maximum power point in A, V_{MPP} is the voltage at maximum power point in V, P_s is the output power of the PV module in W, and N is the number of modules.

B. Reactive Power Capability of Solar DG

In solar DG, reactive power is significantly affected by the characteristics of the inverter and the current and terminal voltage rating [18]. Normally, solar DG inverters are designed to operate at unity power factor [19]. However, with technological advancements, certain inverters now can supply reactive power to the system. By controlling the reactive power of solar DG, voltage fluctuations in the system can be minimized by preventing possible disturbances to the grid [20]. In this study, three different models of reactive power control of solar DG were considered:

1. *Unity Power Factor Model.* This model implies that solar modules are supplying real power only.
2. *Constant Power Factor Model.* This model

follows the allowable utility standards of constant pf of 0.95 either lagging or leading for improved efficiency in delivering real power to the system [12]. In this study, only the production of constant lagging pf in relation to real power of DG is considered, as shown in the equation:

$$Q_{DG} = P_s(s) * \tan(0.95) \quad (9)$$

3. *Variable Lagging Power Factor Model.* For this model, the reactive power is varied depending on the hours of the day. Operators may identify a dynamic range of 0.95 lagging to 0.95 leading with time delay for values less than 0.95 pf [12, 18]. During the time when the resources are low, plants may be disconnected to the grid, causing the DC voltages to limit the reactive power capability of inverters [18].

Wind DG Modelling

The stochastic nature of the wind speed was considered for the wind DG power output. Different reactive power capability were adopted including unity power factor, constant power factor lagging, constant power factor leading, and induction generation wind DG models.

A. Weibull Distribution of Wind Speed

Proper modelling of wind power which includes data fitting and power output derating is necessary to consider the intermittent nature of wind DG. Wind speed data are commonly fitted to a Weibull distribution [17, 21]. The Weibull is represented by the equation:

$$p(v) = \left(\frac{k}{A}\right) \left(\frac{v}{A}\right)^{k-1} e^{-\left(\frac{v}{A}\right)^k} \quad (10)$$

where $p(v)$ is the density function for wind speed, k is the shape parameter; $k > 0$, A is the scale parameter; $A > 0$, and v is the wind speed (m/s); $v > 0$. Moreover, wind power output [21] is computed using the equation.

$$P(v) = \begin{cases} 0 & v < v_c \text{ or } v > v_s \\ P_{rated} \left(\frac{v - v_c}{v_R - v}\right) & v < v_R \\ P_{rated} & v_R \leq v \leq v_s \end{cases} \quad (11)$$

where $P(v)$ is the wind power curve, v_c is the cut-in wind speed in m/s, v_R is the rated speed in m/s, v_s is the cut-out speed in m/s, and v is the wind speed in m/s. For this study, v_c , v_R , v_s [13] are assumed and set to be 2.5 m/s, 14 m/s and 25 m/s, respectively.

B. Reactive Power Capability of Wind DG

A comparison of different models of wind DG allocation reported that the improvement of voltage profile and reduction of power loss in a system varies from one model to another. It was also highlighted that the constant pf lagging model had given the most significant improvement to the system [13]. In this study, four wind DG models were adopted, namely:

1. *Unity Power Factor Model.* This generator is capable of injecting real power only to the system.

$$Q_{DG} = 0 \quad (12)$$

2. *Constant Power Factor Lagging Model.* This generator is capable of injecting both real and reactive powers to the system.

$$Q_{DG} = P_s(s) * \tan(\cos^{-1}0.95) \quad (13)$$

3. *Constant Power Factor Leading Model.* This generator is capable of injecting real power to the system and consuming reactive power.

$$Q_{DG} = -P_s(s) * \tan(\cos^{-1}0.95) \quad (14)$$

4. *Induction Generation Model.* Before injecting real power to the system, this generator initially consumes reactive power.

$$Q_{DG} = -(0.5 + 0.04(P_{DG}^2)) \quad (15)$$

Voltage-Dependent Load Model

The voltage dependent load models affect the characteristics and operations of the distribution system [14]. The voltage dependency of the load is expressed by the following equations:

$$P = P_o \times V_o^\alpha \tag{16}$$

$$Q = Q_o \times V_o^\beta \tag{17}$$

where P and Q are the real and reactive powers at a given voltage level, P_o and Q_o are the real and reactive powers at nominal voltage, and α and β are the real and reactive power exponents. Table 1 shows the typical α and β at different load types.

Table 1. Typical α and β values at different load types

Load type	α	β
Constant	0	0
Residential	0.92	4.04
Commercial	1.51	3.04

Problem Formulation

The optimal allocation of wind and solar DGs has the main objective of minimizing power loss [12], as expressed in equation:

$$F = \min \sum S_{loss} \tag{18}$$

subject to the following constraint:

$$0.90 \leq V_i \leq 1.10 \quad i = 2,3,4, \dots, 37 \tag{19}$$

$$line\ capacity \geq line\ current \tag{20}$$

where F is the objective or fitness function, S_{loss} is the total apparent power loss in kVA, and V_i is the voltage at any bus in pu.

Implementation

The distribution network, loads, and DG were modeled in the OpenDSS. This load flow software is commonly used because of its fast convergence and capability to implement analysis of DG, simulations of PV and wind systems, and

modelling of storage devices [24]. It can also be utilized with other software for simulations through its Component Objective Model (COM) interface.

Using its COM server, it was interfaced with MATLAB where the optimization algorithm was developed. Genetic algorithm (GA) was utilized to get an optimal solution from a pool of samples [25]. The process starts with the coding of the size and site of DG as a single chromosome. In the coding of chromosomes, the size of the DG was considered first followed by the corresponding location of each DG using binary digits. The next step is to initialize the population through random generation of chromosomes. The objective function is evaluated by assigning fitness values to each chromosome. All the members of the population will undergo the iterative process of selection, crossover, and mutation [26]. For this study, GA is set to have 100 populations, 100 generations, single-point crossover, and 5% mutation rate.

Load flow analysis was implemented throughout the day to consider the stochastic nature of both renewable DGs. For the results to be more accurate, 20 samples were generated for each hour utilizing the randomly-selected solar irradiances and wind speeds based on their respective pdf. The power outputs of the wind and solar DGs were then calculated using the wind and solar data, respectively. For each hour, the power loss and phase bus voltages were calculated. The average values of power loss and bus voltages were solved for the objective function [12, 13].

The load flow implementations were done using OpenDSS. All modifications in the network such as integration of DG and load models, and GA optimization were implemented using MATLAB. The solar and wind data were taken from Philippine Atmospheric, Geophysical and Astronomical Services Administration (PAGASA).

DG Site And Size

The IEEE 37-bus test system is a highly-unbalanced system with 25 load buses where loads are considered as spot loads. It has a nominal voltage of 4.8 kV with all the lines configured

as underground connected [27]. Figure 1 shows the single line diagram of the IEEE 37-bus test system. All nodes except the slack bus can be a candidate site for DG siting.

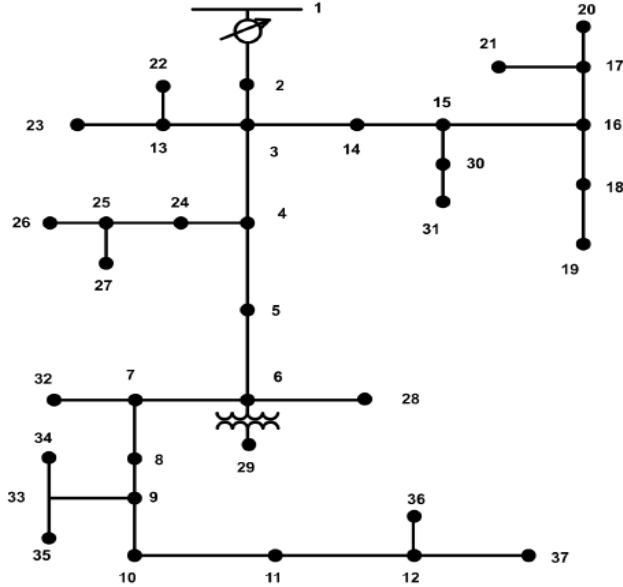


Figure 1. Single line diagram of IEEE 37-bus test system

For wind DG, commercially-available sizes are considered in this study with nominal power rating of 1 kW, 7 kW, 50 kW, 100 kW and 500 kW [28]. Likewise, commercially-available sizes for solar DG are considered with nominal power rating of 240 W, 245 W, 250 W, 255 W, 260 W, and 265 W. Table 2 shows the specifications and sizes of the solar DG module used in the study.

Comparison of Models

Three models of solar DG and four models of wind DG were considered in this study. Each model has three cases corresponding to systems with constant PQ, residential and commercial load models, respectively. The effect of different load models to the optimal allocation of DG were compared for each DG model. The bases of comparison within DG models were the percent reduction in losses and total voltage deviation (TVD). The base case for this study is the system with no DG and with constant PQ load model. For each case in every model, percent power loss reduction [13] was computed using the following equations:

$$\%PLR = \frac{P_{loss,no\ DG} - P_{loss,with\ DG}}{P_{loss,no\ DG}} \times 100 \quad (21)$$

$$\%QLR = \frac{Q_{loss,no\ DG} - Q_{loss,with\ DG}}{Q_{loss,no\ DG}} \times 100 \quad (22)$$

where $\%PLR$ is the active power loss reduction in %, $P_{loss,no\ DG}$ is the active power loss without DG in kW, $P_{loss,with\ DG}$ is the active power loss with DG in kW, $\%QLR$ is the reactive power loss reduction in %, $Q_{loss,no\ DG}$ is the reactive power loss without DG in kVar, $Q_{loss,with\ DG}$ is the reactive power loss with DG in kVar.

In addition, the ideal value for the voltage V at any bus i is equal to 1.0 pu thus the ideal value of TVD is equal to zero. TVD [12] for each solution was quantified using equation (23), where TVD is the Total Voltage Deviation, and V_i is the voltage at the i th bus in pu.

$$TVD = \sum_{i=1}^{37} |V_i - 1| \quad (23)$$

Table 2. Solar DG module sizes and specifications

CHARACTERISTICS	MODULE SIZES (W)					
	240	245	250	255	260	265
Voc (V)	36.45	36.78	37.12	37.45	37.78	38.12
Isc (A)	8.59	8.68	8.76	8.85	8.93	9.01
Vmpp(V)	29.86	30.12	30.38	30.64	30.9	31.16
Impp (A)	8.1	8.2	8.29	8.39	8.48	8.57
NOCT (°C)	46	46	46	46	46	46

Results and Discussion

The effects of load model considerations in the allocation of different solar and wind DG models were evaluated by comparing the results to a base case. Specifically, power losses and voltage profile of each case were compared to a base case.

Base Case

The base case scenario shows that the total real and reactive power losses of the system are 65.02 kW and 50.82 kVar, respectively. For all

phases, buses 12, 36 and 37 corresponds to the location with low bus voltage as shown in Figure 2. The average TVD is 1.11 pu.

Solar DG Integration

Three different load models and solar DG models were considered in the simulation. Table 3 summarizes the optimization results upon the integration of solar DG. In all solar DG models, 265 W, the largest possible size, was found as the optimal DG size. Furthermore, bus 36, the location with lowest recorded voltage at base case as shown in Figure 2, was chosen as the optimal

Table 3. Summary of the optimization results for solar DG

DG Model	Load Model	Size (W)	Bus No.	$P_{loss,red}$ (%)	$Q_{loss,red}$ (%)	TVD (pu)
Unity	Constant PQ	265	36	4.926	5.340	1.087
	Residential	265	36	14.244	15.668	1.021
	Commercial	265	36	16.004	17.629	1.016
Constant Lagging	Constant PQ	265	36	5.727	6.192	1.079
	Residential	265	36	14.881	16.349	1.014
	Commercial	265	36	16.662	18.330	1.010
Variable Lagging	Constant PQ	265	36	5.498	5.948	1.081
	Residential	265	36	14.700	16.154	1.016
	Commercial	265	36	16.425	18.076	1.012

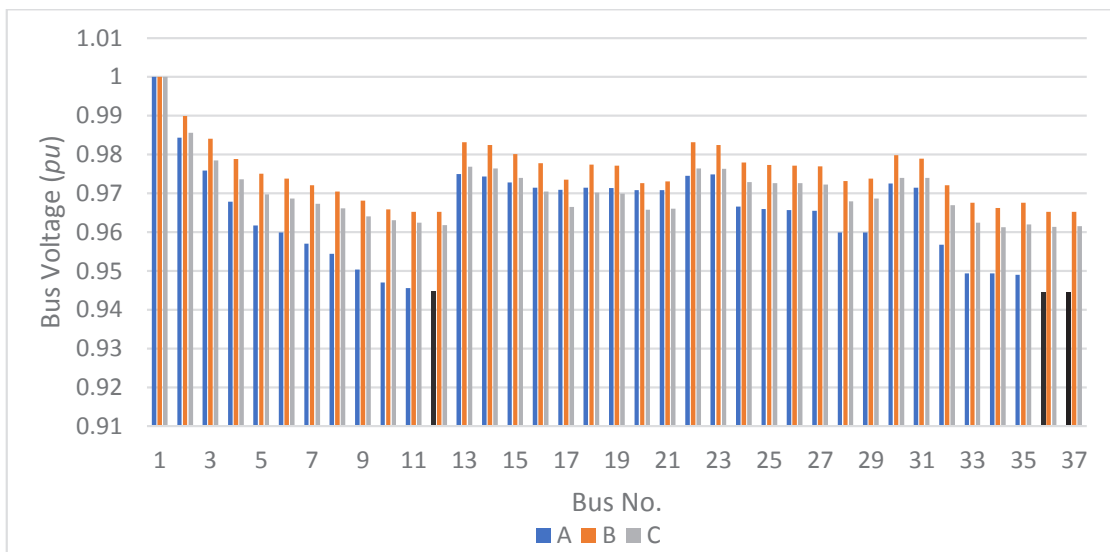


Figure 2. Voltage profile at phase A, B and C of base case scenario

site for all DG models. Installation of DG caused significant reduction in both real and reactive power losses of the system. It can be noted that the maximum real and reactive power loss reductions and the minimum TVD in each model were observed in the system with commercial load model.

The highest loss reductions and least TVD were recorded from the integration at bus 36 of a 265-W constant lagging solar DG with commercial load model. The resulting real and reactive power loss reductions are 16.66% and 18.33%, respectively. Meanwhile, the recorded minimum TVD of the system is 1.010 pu.

Wind DG Integration

The optimization results of different wind DG integration scenarios are presented in Table 4. The optimal locations of DG match the buses of the lowest nodal voltage recorded at the base case as shown in Figure 2. It can be noted that the maximum real and reactive power loss reductions and the minimum TVD in each model were observed in the system with commercial load model.

The highest recorded power loss reduction and voltage profile improvement resulted from the integration at bus 36 of a 500-kW wind DG with constant pf lagging model at a system using commercial load model. The resulting active and reactive power loss reductions were 13.88% and 15.30%, respectively. Meanwhile, the recorded minimum TVD of the said system is 1.024 pu. It can also be observed that only induction model generator has the optimal size that is equal to 100 kW. This means that injecting 500 kW to the system results in higher apparent loss compared with the system with 100 kW. Furthermore, as shown in Figure 3, it can be observed that the resulting apparent loss while injecting 500 kW exceeds the base case apparent loss.

Power Losses

Comparisons of system power losses of different solar and wind DG integration scenarios are presented in Figure 4. It can be deduced from the data that in each DG model, for both solar and wind, the system with commercial load model consideration yielded the lowest real and reactive power loss.

Table 4. Summary of the optimization results for wind DG

DG Model	Load Model	Size (kW)	Bus No.	$P_{\text{loss,red}}$ (%)	$Q_{\text{loss,red}}$ (%)	TVD (pu)
Unity	Constant PQ	500	36	2.240	2.416	1.098
	Residential	500	36	11.776	12.978	1.032
	Commercial	500	36	13.573	14.975	1.027
Constant Lagging	Constant PQ	500	36	2.617	2.816	1.095
	Residential	500	37	12.070	13.299	1.029
	Commercial	500	36	13.881	15.303	1.024
Constant Leading	Constant PQ	500	12	1.872	2.034	1.103
	Residential	500	36	11.486	12.673	1.037
	Commercial	500	36	13.331	14.724	1.031
Induction	Constant PQ	100	36	0.428	0.460	1.111
	Residential	100	36	10.100	11.169	1.044
	Commercial	100	37	11.940	13.211	1.040

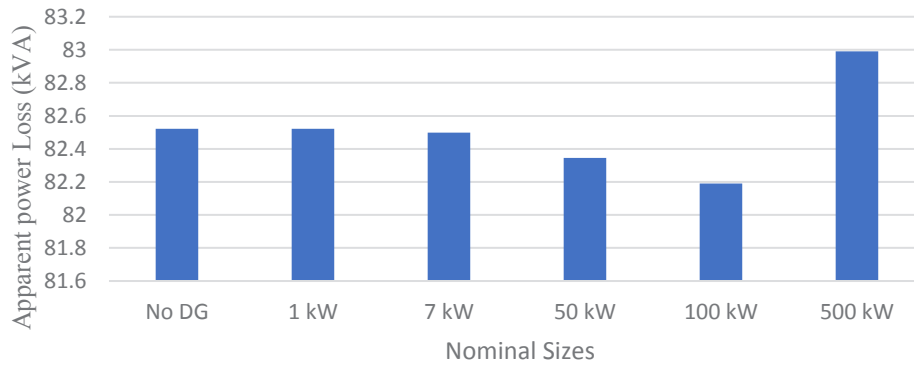


Figure 3. Apparent Power Loss for different sizes of Induction Model Generator

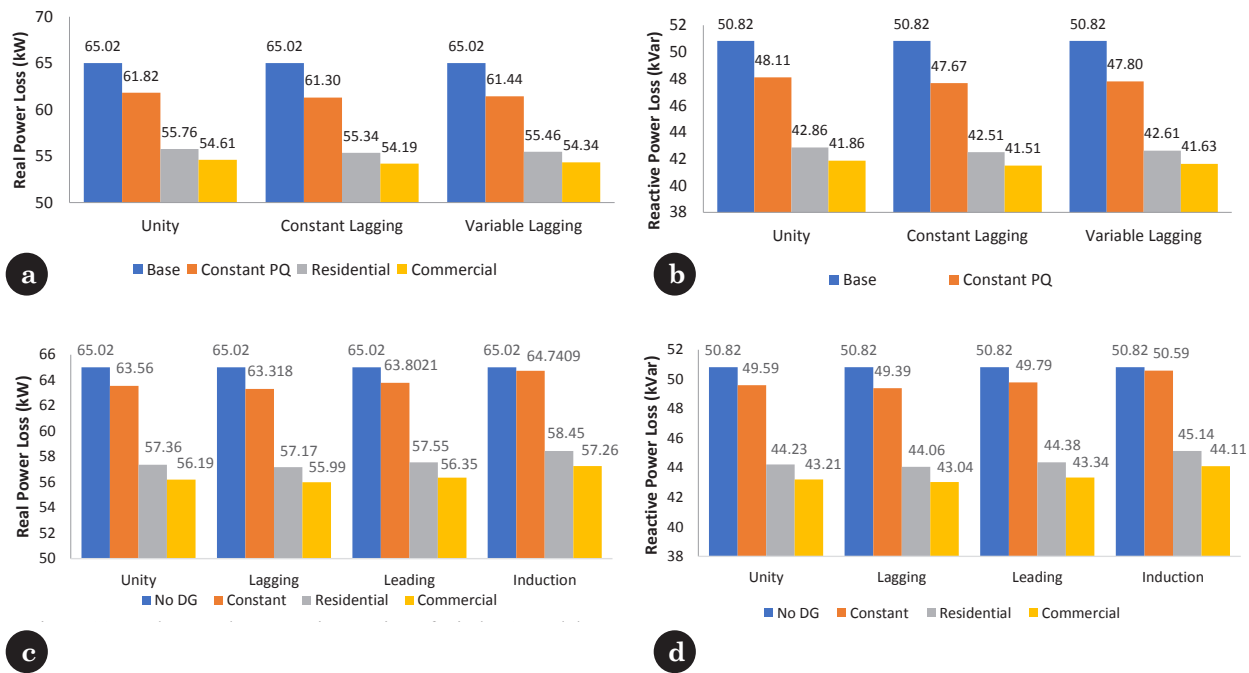


Figure 4. (a) Real power loss upon integration of solar DG models (b) Reactive power loss upon integration of solar DG models (c) Real power loss upon integration of wind DG models (d) Reactive power loss upon integration of wind DG models

The lowest power losses for both types of DG were observed from the integration of a constant lagging DG model with commercial load model. For solar DG, the lowest recorded active and reactive losses were 54.19 kW and 41.51 kVar, respectively. For wind DG, on the other hand, the resulting real and reactive losses were 55.99 kW and 43.04 kVar, respectively.

Inclusion of different DG models in the analysis significantly affects both real and reactive power loss of the system. Considering the effect of load models, it is observed that for constant lagging solar DG, the residential load yielded a 10.16% difference as compared to the system with constant PQ model. However, 12.14% difference is observed for commercial load model,

which is considerably larger as compared to residential, showing that it has a greater impact on the system in terms of loss reduction. As for constant pf lagging wind DG, the residential load resulted in a 10.48% difference when compared to the system with constant PQ load model while the commercial load yielded a difference of 12.49%.

Voltage Profile

A sample voltage profile at phase A of unity solar and wind DG models are illustrated in Figures 5 and 6. It can be observed that integrating

the load model to the system intensifies the improvement of the system voltage. Moreover, with the integration of solar and wind DG, the voltage profile improved considerably especially in buses with low voltage such as buses 10, 11, 12, 36 and 37. However, the most improved nodal voltages are located in the point of integration of the DGs. Similar results were observed for the other DG models and phase voltages.

For solar DG, integrating the constant pf lagging to a system with commercial load model caused the most significant improvement in the voltage profile of the system. Same observation was recorded for the wind DG.

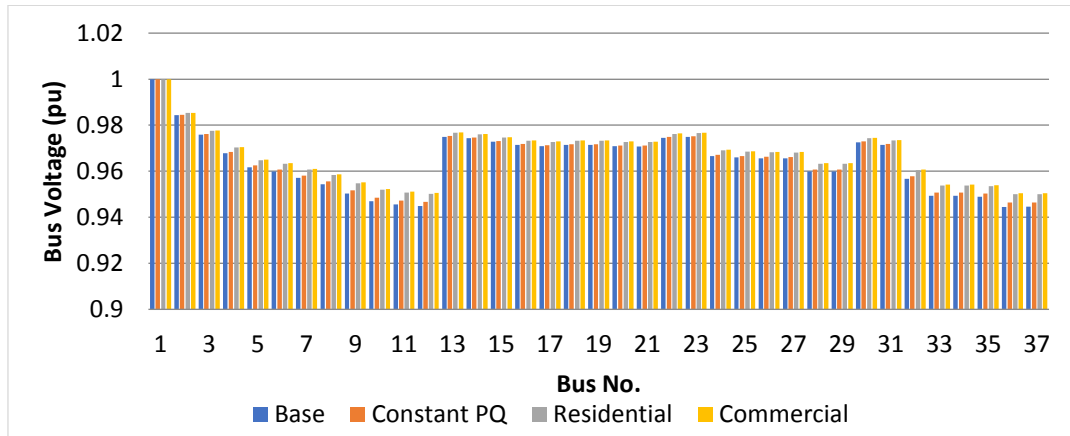


Figure 5. Voltage profile at phase A of unity solar DG model

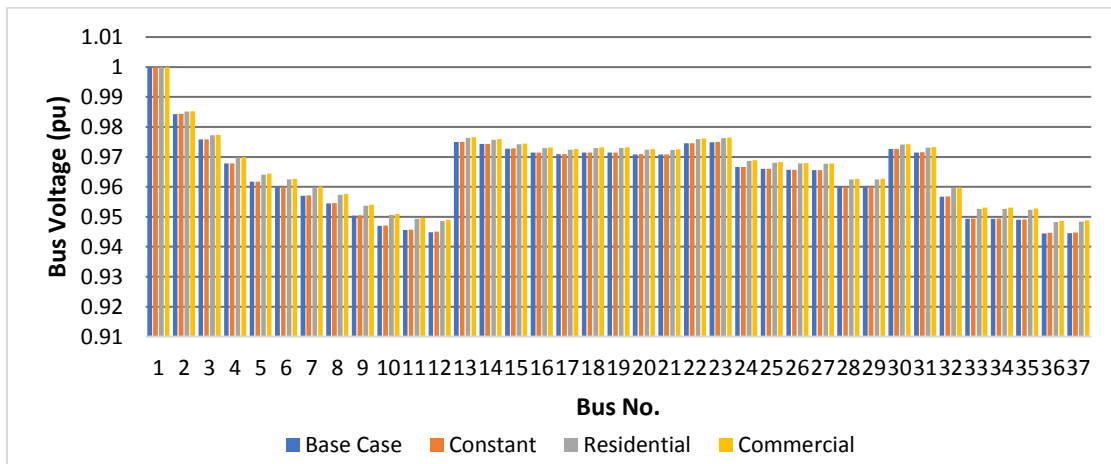


Figure 6. Voltage profile at phase A of unity wind DG model

Conclusion

Inclusion of DG reactive capability and load models in the analyses significantly affect the power loss and voltage profile of the system. For each DG model, the system with commercial type of load resulted in the highest loss reduction while least loss reduction was found for constant PQ load model. The constant lagging model of both solar and wind DGs with commercial load consideration yielded the lowest active and reactive power losses and best voltage profile improvement. For the constant lagging type of renewable, the computed power loss reduction for the residential load differs by as much as 10.16% and 10.48% for solar and wind, respectively. Meanwhile, the computed power loss reduction for the commercial load deviates by as much as 12.14% and 12.49% for solar and wind, respectively.

For residential and commercial load models, the constant lagging power factor for both solar and wind DG models are viable options in terms of power loss reduction. With the result of this study, distribution network planners can maximize the benefits of integrating DG in the system by properly selecting the type of DG depending on the type of consumers connected.

Acknowledgments

The authors acknowledge the support of the University of the Philippines Los Baños.

References

- [1] U.S. Energy Information Administration, "International Energy Outlook 2016," [Online]. Available: [https://www.eia.gov/outlooks/ieo/pdf/0484\(2016\).pdf](https://www.eia.gov/outlooks/ieo/pdf/0484(2016).pdf). [Accessed: 14-Dec-2017].
- [2] Department of Energy and Electric Power Industry Management Bureau, "Power Supply and Demand Highlights (January-June 2017)," [Online]. Available: https://www.doe.gov.ph/sites/default/files/pdf/electric_power/power_supply_demand_highlights_jan_jun_2017.pdf. [Accessed: 25-Aug-2018].
- [3] K. B. Reddy, K. H. Reddy, and P. S. Babu, "Optimal Location and Size of Distributed Generations Using Kalman Filter Algorithm for Reduction of Power Loss and Voltage Profile Improvement," *International Journal of Engineering Research and Development*, vol. 10, no. 9, pp. 19-28, 2014.
- [4] T. J. Sahib, M. R. Ab. Ghani, Z. Jano, and I. H. Mohamed, "Optimum Allocation of Distributed Generation using PSO: IEEE Test Case Studies Evaluation," *International Journal of Applied Engineering Research*, vol. 12, no. 11, pp. 2900–2906, 2017.
- [5] D. Rama Prabha and T. Jayabarathi, "Optimal placement and sizing of multiple distributed generating units in distribution networks by invasive weed optimization algorithm," *Ain Shams Engineering Journal*, vol. 7, no. 2, pp. 683–694, 2016.
- [6] M. Shahzad, I. Ahmad, W. Gawlik, and P. Palensky, "Load Concentration Factor Based Analytical Method for Optimal Placement of Multiple Distribution Generators for Loss Minimization and Voltage Profile Improvement," *Energies*, vol. 9, no. 4, pp. 1-21, 2016.
- [7] P. Sharma and A. Tandon, "Techniques for optimal placement of DG in radial distribution system: A review," in *2015 Communication, Control and Intelligent Systems (CCIS)*, 2015, pp. 453–458.
- [8] IRENA, "Renewable Power Generation Costs in 2017," *International Renewable Energy Agency*, 2018. [Online]. Available: https://www.irena.org/-/media/Files/IRENA/Agency/Publication/2018/Jan/IRENA_2017_Power_Costs_2018.pdf. [Accessed: 02-Feb-2019].
- [9] F. Rezaei and S. Esmaili, "Decentralized reactive power control of distributed PV and wind power generation units using an optimized fuzzy-based method," *International Journal of Electrical Power & Energy Systems*, vol. 87, pp. 27–42, 2017.
- [10] G.V.N. Lakshmi, A.J. Laxmi, and V.V. Reddy, "Optimal Allocation and Sizing of Multiple Distributed Generators Using

- Genetic Algorithm,” in *International Conference on Advances in Communication, Network, and Computing*, 2014, pp. 305–312.
- [11] S. Remha, S. Chettih, and S. Arif, “Optimal placement of different DG units type in distribution networks based on voltage stability maximization and minimization of power losses,” in *2016 8th International Conference on Modelling, Identification and Control (ICMIC)*, 2016, pp. 867–873.
- [12] J. K. L. Caasi and R. A. Aguirre, “Comparative analysis of the optimal siting and sizing on different solar distributed generation models through stochastic method,” in *2016 IEEE Innovative Smart Grid Technologies - Asia (ISGT-Asia)*, 2016, pp. 485–490.
- [13] L. D. T. Narcise and R. A. Aguirre, “Comparative analysis of optimal allocation for different wind distributed generation models using stochastic approach,” in *2016 IEEE Innovative Smart Grid Technologies - Asia (ISGT-Asia)*, 2016, pp. 46–51.
- [14] H. Nasiraghdam and S. Jadid, “Load model effect assessment on optimal distributed generation (DG) sizing and allocation using improved harmony search algorithm,” in *2013 Smart Grid Conference (SGC)*, 2013, pp. 210–218.
- [15] D. Singh, D. Singh, and K. S. Verma, “Multiobjective Optimization for DG Planning With Load Models,” *IEEE Transactions on Power Systems*, vol. 24, no. 1, pp. 427–436, 2009.
- [16] H. Qamar, H. Qamar, A. Vaccaro, and N. Ahmed, “Reactive power control for voltage regulation in the presence of massive pervasion of distributed generators,” in *2017 IEEE International Conference on Environment and Electrical Engineering and 2017 IEEE Industrial and Commercial Power Systems Europe (EEEIC / I&CPS Europe)*, 2017, pp. 1–5.
- [17] Y. M. Atwa, E. F. El-Saadany, M. M. A. Salama, and R. Seethapathy, “Optimal Renewable Resources Mix for Distribution System Energy Loss Minimization,” *IEEE Transactions on Power Systems*, vol. 25, no. 1, pp. 360–370, 2010.
- [18] A. Ellis, R. Nelson, E. Von Engeln and R. Walling, “Reactive power performance requirements for wind and solar plants,” in *2012 IEEE Power and Energy Society General Meeting*, 2012, pp. 1–8.
- [19] G. J. Shirek and B. A. Lassiter, “Solar plant modeling impacts on distribution systems PV case study,” in *2012 Rural Electric Power Conference*, 2012, pp. B5-1-B5-10.
- [20] Y. Zhang, S. Zhu, R. Sparks, and I. Green, “Impacts of solar PV generators on power system stability and voltage performance,” in *2012 IEEE Power and Energy Society General Meeting*, 2012, pp. 1–7.
- [21] M. Alotaibi, A. Almutairi, and M. M. A. Salama, “Effect of wind turbine parameters on optimal DG placement in power distribution systems,” in *2016 IEEE Electrical Power and Energy Conference (EPEC)*, 2016, pp. 1–4.
- [22] P. Wais, “Two and three-parameter Weibull distribution in available wind power analysis,” *Renewable Energy*, vol. 103, pp. 15–29, 2017.
- [23] V. Gupta, S. R. Donepudi, and N. Subrahmanyam, “Optimal placement of distributed generators in distribution system using backtracking search optimization for various load models,” in *2015 International Conference on Recent Developments in Control, Automation and Power Engineering (RDCAPE)*, 2015, pp. 350–354.
- [24] Electric Power Research Institute, “Simulation Tool - Open DSS,” [Online]. Available: <http://smartgrid.epri.com/SimulationTool.aspx>. [Accessed: 20-April-2018].
- [25] G. Lindfield and J. Penny, *Introduction to Nature-Inspired Optimization*, Academic Press, 2017.
- [26] K. Deep and M. Thakur, “A new mutation operator for real coded genetic algorithms,” *Applied Mathematics and Computation*, vol. 193, no. 1, pp. 211–230, 2007.
- [27] W. H. Kersting, “Radial distribution test feeders,” *IEEE Transactions on Power Systems*, vol. 6, no. 3, pp. 975–985, 1991.
- [28] K. Corfee, G. Stevens, and S. Goffri, “Distributed Generation Resource

Assessment for Long-Term Planning Study,” [Online]. Available: http://www.pacificorp.com/content/dam/pacificorp/doc/Energy_Sources/Integrated_Resource_Plan/2015IRP/2015IRPStudy/Navigant_Distributed-Generation-Resource-Study_06-09-2014.pdf. [Accessed: 25-June-2018].

- [29] Astronergy, “Datasheet Crystalline PV Module ASM6610P Series,” [Online]. Available: http://www.astronergy.com/attach/product/ASM6610P_US201507.pdf. [Accessed: 12-Mar-2018].